In-Flight Alignment in INS-Aiding with Switched Feedforward/Feedback of Error Estimates

Jacques Waldmann
Department of Systems and Control, Instituto Tecnológico de Aeronáutica, 12228-900, São José dos Campos, Brasil.

***Abstract* — Unmanned air vehicles often resort to a low-cost inertial measurement unit (IMU) in an inertial navigation system (INS) to estimate position and velocity. Stand-alone INS operation yields unbounded estimation errors. Such behavior motivates INS aiding by auxiliary position and velocity sensors to limit navigation error. Acceleration maneuvers and IMU rotation with respect to the vehicle are used to enhance the observability of INS error dynamics, in conjunction with Kalman filter-based sensor fusion to estimate position and velocity errors, IMU misalignment and sensor errors. This work investigates feedforward and feedback of error estimates for INS aiding. Feedforward integration is used to estimate IMU misalignment and sensor errors with adequate accuracy, and then switches to feedback integration for in-flight alignment (IFA), that is INS reset and IMU calibration during operation. A Monte Carlo simulation provides evidence supporting the approach.**

***Keywords* — inertial navigation, in-flight alignment, sensor fusion,autonomous vehicles, robotics.**

I. INTRODUCTION

An inertial navigation system (INS) estimates position and velocity. Gimbaled INS implementations (GINS) employ accurate mechanisms to isolate the IMU from the host vehicle's motion and keep alignment with the navigation reference frame. A strapdown configuration (SDINS) employs an IMU rigidly attached to the host vehicle. The INS can track short-term, abrupt motions, but estimation errors grow unbounded during long operation periods due to the integration of low-frequency errors such as accelerometer bias and rate-gyro drift, which are here assumed to be unknown, constant null offsets. Before entering navigation mode, IMU calibration and alignment – often relative to the North-East-Down frame – make use of leveling and gyrocompassing while the vehicle remains stationary at a known location on the ground. More recently, autonomous vehicles resort to a low-cost SDINS aided by additional sensors, and Kalman filter-based sensor fusion is employed to estimate navigation, IMU misalignment and sensor errors [1]-[5].

Reference [6] showed the lack of full observability when estimating IMU misalignment and sensor errors of a stationary GINS with velocity error measurements. Their analysis employed linear navigation and misalignment error dynamics augmented with random constant accelerometer bias and rate-gyro drift. Reference [7] departed from the augmented computer-frame velocity error model of a GINS, investigated its observability, and indicated that the ability to maneuver is "a blessing in disguise". That is, though IFA may seem to be less accurate and more complicated than alignment at rest, maneuvers during the IFA phase can excite latent error dynamics. Acceleration maneuvers in a GINS were modeled by a concatenation of piece-wise constant (PWC) specific force segments to circumvent the trajectory-dependent, numerical computation of the observability Grammian of a linear time-varying model. Observability analysis of the PWC linear error dynamics was based on determining the rank of the stripped observability matrix (SOM) after each acceleration segment [7][8]. However, SOM analysis disregarded the actual model mismatch arising from linearization errors during operation and its effect on error estimation accuracy.

Reference [7] claimed further that covariance simulation and real IFA results showed that the exact nature of acceleration maneuvers is not influential, but their mere existence is paramount for accurate GINS misalignment and IMU error estimation. Thus, insights from SOM analysis seem to apply to other GINS-equipped vehicles and maneuvers. On the other hand, most SDINS-equipped vehicles conduct attitude maneuvers to generate accelerations. It is intuitive that maneuvers in acceleration *and* IMU attitude should enhance estimation accuracy, but continuously changing IMU attitude violates the assumption of PWC dynamics, which precludes SOM analysis.

Instead of a strapdown configuration, here the IMU rotates relative to the host vehicle. IMU rotation does not require the accurate mechanism of a gimbaled INS because what matters is to change the direction of the inertial sensors' sensitive axes relative to gravity and earth angular rate. Hence, the host vehicle need not maneuver away from the desired path for observability enhancement during IFA. The IMU can be locked in a known attitude relative to the vehicle following the IFA phase. The approach has been inspired by [8], which employed SOM analysis and concatenated PWC segments of IMU attitude for multiposition alignment on the ground. Notice that vehicle attitude is a by-product of the conventional strapdown configuration at all times, whereas during IFA phase the present approach produces IMU attitude. The inertial sensors are assumed to be aligned with the IMU frame S_b.

The second purpose of this investigation is to evaluate both feedforward and feedback of navigation and IMU sensor error estimates based on aiding position and velocity sensors

J. Waldmann, jacques@ita.br, Tel +55-12-39475993, Fax +55-12-39475878
This research has been partially supported by project FINEP/CTA/INPE Inertial Systems for Aerospace Application (SIA). A similar manuscript has been submitted to V SBEIN 2007 - Simpósio Brasileiro de Engenharia Inercial - and is presently undergoing peer review.

for sensor fusion. Feedforward aiding employs a Kalman filter linearized about the diverging INS estimates, and removes *a posteriori* the estimated position and velocity errors from the INS output. On the other hand, feedback aiding employs in-flight INS reset and IMU calibration, thus resulting in an extended Kalman filter linearized about the corrected INS output. This work initially resorts to feedforward fusion to estimate misalignment and IMU errors with sufficient accuracy, and then switches to feedback fusion for INS reset and IMU calibration.

II. INERTIAL NAVIGATION AND ATTITUDE DETERMINATION

The continuous-time navigation equations in the local North-East-Down reference frame S_{NED} are:

$$\dot{\lambda} = \frac{V_N}{R_N + h} \;; \quad \dot{\Lambda} = \frac{V_E}{(R_E + h)\cos(\lambda)} \;; \quad \dot{h} = -V_D$$

$$\dot{V}_N = A_{sp,N} + \frac{V_N V_D}{(R_N + h)} - V_E\{2\Omega\sin(\lambda) + \frac{V_E \tan(\lambda)}{(R_E + h)}\}$$

$$\dot{V}_E = A_{sp,E} + V_N\{2\Omega\sin(\lambda) + \frac{V_E \tan(\lambda)}{(R_E + h)}\} + V_D\{2\Omega\cos(\lambda) + \frac{V_E}{(R_E + h)}\}$$

$$\dot{V}_D = A_{sp,D} - \frac{V_N V_N}{(R_N + h)} - V_E\{2\Omega\cos(\lambda) + \frac{V_E}{(R_E + h)}\} + g(\lambda, h)$$

$$g(\lambda, h) = g_0(1 + 0.0053\sin^2(\lambda))(1 - 2h / R_e) \qquad (1)$$

Latitude λ, longitude Λ, and altitude h describe the terrestrial position, whereas V_N, V_E, and V_D are the North, East, and Down components of velocity relative to Earth rotating with rate Ω. The U.S. Department of Defense World Geodetic System (DoD WGS-84) approximates the earth's shape by a geocentric reference ellipsoid, which models earth radius $R_e(\lambda)$, curvature radii $R_E(\lambda)$ and $R_N(\lambda)$ along East and North directions, respectively, and gravity [9]. Gravity magnitude model $g(\lambda,h)$ is a sufficiently accurate approximation of gravity for the present purposes [10].

Use of accelerometer data in (1) needs attitude determination, i.e. the transformation from S_b to S_{NED}. One approach is to compute the direction cosine matrix (DCM) from angular rate measurements and the initial alignment's DCM:

$$\dot{\mathbf{D}}^{b}_{NED,INS} = \mathbf{D}^{b}_{NED,INS}\boldsymbol{\Omega}^{bi}_{b,m} - \boldsymbol{\Omega}^{NEDi}_{NED,INS}\mathbf{D}^{b}_{NED,INS} \qquad (2)$$

The subscript m indicates a measured value, whereas *INS* means the INS stand-alone solution. The entries in skew-symmetric matrix $\boldsymbol{\Omega}^{bi}_{b,m}$ are the S_b components of the angular rate sensed by the IMU's rate-gyro triad. Likewise, skew symmetric matrix $\boldsymbol{\Omega}^{NEDi}_{NED,INS}$ relates to the components of $\boldsymbol{\omega}^{NEDi}_{NED,INS}$ according to:

$$\boldsymbol{\omega}^{NEDi}_{NED,INS} = [(\Omega + \dot{\Lambda}_{INS})\cos(\lambda_{INS}) \quad -\dot{\lambda}_{INS} \quad -(\Omega + \dot{\Lambda}_{INS})\sin(\lambda_{INS})]^T \qquad (3)$$

$\dot{\Lambda}_{INS}, \dot{\lambda}_{INS}, \lambda_{INS}$ are from the INS stand-alone solution to (1). The INS stand-alone solution to (1) and (2) is computed by a multirate algorithm to reduce the computational burden. The algorithm processes IMU discrete-time measurements, that is angular and thrust velocity increments occurring between sensor samples [11]-[13][16]. Coning errors arise because finite rotations do not commute, sculling errors are due to incorrect thrust velocity computation as coordinate frames rotate between data samples, and scrolling errors arise from velocity and position updates occurring at distinct rates. Though complex, with intricate compensation terms to attenuate such errors, the multirate approach in [12] was utilized due to its enhanced accuracy. Thrust velocity increments from the accelerometers are transformed from S_b to S_{NED} at a high sampling rate, and terrestrial velocity and position are solved at intermediate and slow rates, respectively. The fast acquisition rate of incremental inertial samples and attitude computation has been set to 400Hz. The INS terrestrial velocity and position are computed at the intermediate and slow rates $1/T_{int}$=200Hz and $1/T_{nav}$=100Hz, respectively. The stand-alone inertial solution diverges due to errors in IMU data and erroneous processing by the multirate algorithm, thus causing linearization errors and model mismatch in the Kalman filter used for fusion of the INS solution with aiding sensors.

Fig. 1 shows the most relevant NED coordinate frames and misalignment angles in modeling the error dynamics for Kalman filter-based sensor fusion. True, computed, and platform frames, S_t, S_c, and S_p, respectively, are located at the actual and estimated positions. S_c is perfectly known, albeit it is incorrect.

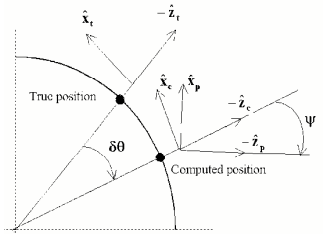

Fig. 1. NED coordinate frames and respective misalignment angles

If initial alignment and inertial data were error free, integration of (2) would produce $\boldsymbol{D}^{b}_{t}$. However, accelerometer bias and rate-gyro drift yield $\boldsymbol{D}^{b}_{p} = \boldsymbol{D}^{b}_{NED,INS}$. $\boldsymbol{\delta\theta}$ is a small misalignment angle vector due to errors in the estimated position. $\boldsymbol{\delta\theta}$ rotates S_t into alignment with S_c. The small misalignment angle vector $\boldsymbol{\psi}$ is due to rate-gyro drift, and rotates S_c into alignment with S_p. Use of the computer frame S_c for the error model is attractive because it renders the misalignment rate $\dot{\boldsymbol{\psi}}^{c}$ uncoupled from both position and terrestrial velocity errors. Total misalignment angle $\boldsymbol{\phi}=\boldsymbol{\delta\theta}+\boldsymbol{\psi}$ from S_t to S_p can be estimated using the INS solution to (1), and the Kalman filter estimates of $\boldsymbol{\psi}$ and position error $\boldsymbol{\Delta R}$.

Assuming a spherical earth and the IMU path in the vicinity of the earth's surface, the computer-frame position error model was obtained and further elaborated to show its equivalence to the computer-frame velocity error model [14]. The latter describes the error dynamics with a structure

$\dot{\Delta\mathbf{x}} = \mathbf{A}(t)\Delta\mathbf{x} + \mathbf{n}$ that fits in with the Kalman filter framework where $\mathbf{n}$ is white noise. IMU sensor errors are additive accelerometer bias $\nabla_\mathbf{b}$, rate-gyro drift $\boldsymbol{\varepsilon}_\mathbf{b}$, and white noise:

$$\Delta\mathbf{x} = \left[\Delta\mathbf{R}_{\mathbf{NED}}{}^{T} \quad \Delta\mathbf{V}_{\mathbf{e,NED}}{}^{T} \quad \boldsymbol{\psi}_{\mathbf{NED}}{}^{T} \quad \nabla_\mathbf{b}{}^{T} \quad \boldsymbol{\varepsilon}_\mathbf{b}\right]^{T}$$

$$\Delta\mathbf{R}_{\mathbf{NED}} = \left[\Delta R_N \quad \Delta R_E \quad \Delta R_D\right]^{T} \quad \Delta\mathbf{V}_{\mathbf{e,NED}} = \left[\Delta V_N \quad \Delta V_E \quad \Delta V_D\right]^{T}$$

$$\boldsymbol{\psi}_{\mathbf{NED}} = \left[\psi_N \quad \psi_E \quad \psi_D\right]^{T}$$

$$\nabla_\mathbf{b} = \left[\nabla_{Xb} \quad \nabla_{Yb} \quad \nabla_{Zb}\right]^{T} \quad \boldsymbol{\varepsilon}_\mathbf{b} = \left[\varepsilon_{Xb} \quad \varepsilon_{Yb} \quad \varepsilon_{Zb}\right]^{T}$$

$$\mathbf{A} = \left[\begin{array}{c|c|c|c|c} \mathbf{A_{11}} & \mathbf{I}_3 & \mathbf{0}_3 & \mathbf{0}_3 & \mathbf{0}_3 \\ \hline \mathbf{A_{21}} & \mathbf{A_{22}} & \mathbf{A_{23}} & \mathbf{D}_\mathbf{p}^\mathbf{b} & \mathbf{0}_3 \\ \hline \mathbf{0}_3 & \mathbf{0}_3 & \mathbf{A_{33}} & \mathbf{0}_3 & -\mathbf{D}_\mathbf{p}^\mathbf{b} \\ \hline \mathbf{0}_3 & \mathbf{0}_3 & \mathbf{0}_3 & \mathbf{0}_3 & \mathbf{0}_3 \end{array}\right]$$

$$\mathbf{A_{11}} = \begin{bmatrix} 0 & \rho_D & -\rho_E \\ -\rho_D & 0 & \rho_N \\ \rho_E & -\rho_N & 0 \end{bmatrix} \quad \mathbf{A_{21}} = \mathrm{diag}\left(-g_0/R_0, -g_0/R_0, 2g_0/R_0\right)$$

$$\mathbf{A_{22}} = \begin{bmatrix} 0 & \rho_D + 2\Omega_D & -\rho_E \\ -(\rho_D + 2\Omega_D) & 0 & \rho_N + 2\Omega_N \\ \rho_E & -(\rho_N + 2\Omega_N) & 0 \end{bmatrix}$$

$$\mathbf{A_{23}} = \begin{bmatrix} 0 & -A_{sp,D} & A_{sp,E} \\ A_{sp,D} & 0 & -A_{sp,N} \\ -A_{sp,E} & A_{sp,N} & 0 \end{bmatrix}_m$$

$$\mathbf{A_{33}} = \begin{bmatrix} 0 & \rho_D + \Omega_D & -\rho_E \\ -(\rho_D + \Omega_D) & 0 & \rho_N + \Omega_N \\ \rho_E & -(\rho_N + \Omega_N) & 0 \end{bmatrix} \tag{4}$$

III. INDIRECT FEEDFORWARD/FEEDBACK INS AIDING WITH MANEUVERS FOR IFA ENHANCING

The continuous lines in Fig. 2 depict a feedfoward, indirect Kalman filter-based fusion of INS estimates with aiding position and terrestrial velocity. The term "indirect" refers to error state estimation rather than estimation of the full state. The dashed lines indicate the feedback configuration, in which the INS is reset during operation by subtracting the estimates of misalignment and IMU errors. Noting that subscript *a* indicates aiding sensor, and measurement $\boldsymbol{y}$ is the difference between the INS solution and the aiding position and velocity, then:

$$\mathbf{R_{INS}} = \mathbf{R} + \Delta\mathbf{R}, \quad \mathbf{V_{e,INS}} = \mathbf{V_e} + \Delta\mathbf{V_e}$$

$$\mathbf{y} = \begin{bmatrix} \mathbf{R_{INS}} - \mathbf{R_a} \\ \mathbf{V_{e,INS}} - \mathbf{V_{e,a}} \end{bmatrix} = \begin{bmatrix} \Delta\mathbf{R} - \boldsymbol{\mu} \\ \Delta\mathbf{V_e} - \boldsymbol{\eta} \end{bmatrix} \tag{5}$$

Representation of the above aiding differences in the NED coordinate frame yields:

$$\Delta R_N = (\lambda_{INS} - \lambda_a)(R_N + h_a)$$

$$\Delta R_E = (\Lambda_{INS} - \Lambda_a)(R_E + h_a)\cos(\lambda_a)$$

$$\Delta R_D = -(h_{INS} - h_a)$$

$$\Delta\mathbf{V}_{\mathbf{e,NED}} = (\mathbf{V}_{\mathbf{e,INS}} - \mathbf{V}_{\mathbf{e,a}})_{\mathbf{NED}} = \left[\Delta V_N \quad \Delta V_E \quad \Delta V_D\right]^{T} \tag{6}$$

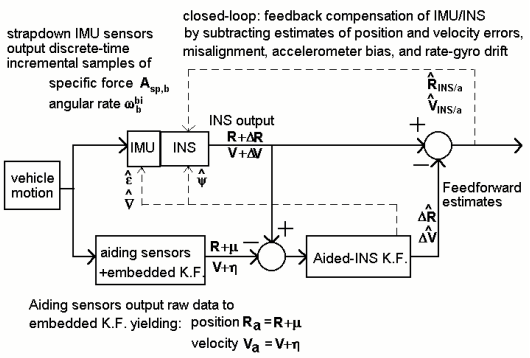

Fig 2. Indirect feedforward INS-aiding architecture. **V** is short for $\mathbf{V_e}$.

Ideally, $\boldsymbol{\mu}$ and $\boldsymbol{\eta}$ are white and uncorrelated noise processes in the aiding sensors. However, the actual processing of observables within the aiding sensors gives rise to correlation in time and among components of aiding position and velocity. Such correlations are not considered here in the statistical model of measurement errors. Thus, the discrete-time measurement equation in the aided-INS Kalman filter is $\boldsymbol{y_j}=[\boldsymbol{\Delta R_{NED}(j)}^T\ \boldsymbol{\Delta V_{e,NED}(j)}^T]^T=\boldsymbol{H\Delta x_j}+\boldsymbol{v_j}$, where $\boldsymbol{v_j}$ is a zero-mean, white sequence with diagonal covariance $\overline{\boldsymbol{R}}$, and $\boldsymbol{H}=diag(\boldsymbol{I_6}, \boldsymbol{O_{6x9}})$.

Measurements $\boldsymbol{A_{sp,NED,m}}$, and INS solution-dependent parameters $\boldsymbol{V_{e,INS}}$, $\boldsymbol{R_{INS}}$ and $\mathbf{D}_{\mathbf{p,INS}}^{\mathbf{b}}$ for use in the Kalman filter have been updated at rate $1/T_{nav}=100Hz$. $\boldsymbol{A(t)}$ has been discretized to produce the state transition matrix, that is $\boldsymbol{\Phi_k} = \boldsymbol{I} + \boldsymbol{A}(kT_{nav})T_{nav}(\boldsymbol{I} + \boldsymbol{A}(kT_{nav})T_{nav}/2)$. Uncertainty in $\boldsymbol{\Phi_k}$ has been translated into an additive, zero-mean, white noise sequence $\boldsymbol{w_k}$ with diagonal covariance matrix $\boldsymbol{Q}$, which is related to the linearization error about the diverging INS solution. Filter estimates and respective covariance matrix have been propagated forward in time also with frequency $1/T_{nav}$. Their updates at rate $1/T_a = 1Hz$ occurred when aiding measurements became available.

Due to model mismatch caused by errors in the INS stand-alone solution, the residual sequence at instants multiple of T_a was monitored to ensure statistical consistency [15]. Adequate tuning of $\boldsymbol{Q}$ should produce a zero-mean, white, Gaussian residual sequence with known covariance matrix $\boldsymbol{S}$. Had a position or velocity residual component been found outside ±3 times the square root of the corresponding element in the diagonal of $\boldsymbol{S}$, the corresponding position or velocity error variance was reset. The corresponding off-diagonal elements in the estimation error covariance matrix were also altered to keep the cross-correlation coefficients unchanged by the reset.

Goshen-Meskin and Bar-Itzhack [7] modeled maneuvers during the IFA phase of a GINS with 20 seconds, piece-wise constant (PWC), 0.1g specific force segments. Consequently, $\mathbf{D}_\mathbf{p}^\mathbf{b} = \mathbf{I}$, and $\boldsymbol{A_{23}}$ in Eq. (5) was the single PWC, significantly time-varying block in $\mathbf{A}(t)$. IMU rotation, however, violates conditions for valid SOM analysis because $\mathbf{D}_\mathbf{p}^\mathbf{b}$ varies continuously. Aiding position and velocity measurements, respectively $\mathbf{R_a}$ and $\mathbf{V_{e,a}}$, have been generated from ground-truth corrupted by additive Gaussian, zero-mean, white noise with a diagonal covariance matrix $\overline{\mathbf{R}}$. IMU rotation with

respect to the vehicle was simulated with IMU attitude ground-truth in terms of yaw, pitch, and roll relative to the NED coordinate frame [11][16]:

$$\begin{aligned}\psi &= s(2\pi t/300) + 0.5\,s(2\pi t/1.7)[rd]\\ \theta &= s(2\pi t/300) + 0.5\,s(2\pi t/1.7 + 0.3)[rd]\\ \phi &= s(2\pi t/300) + 0.5\,s(2\pi t/0.85)[rd] \quad t \in [0,200][s]\end{aligned} \tag{7}$$

The GINS stand-alone solution was simulated by enforcing that $\psi \equiv \theta \equiv \phi \equiv 0$, generating IMU data, and solving Eq. (1) and Eq. (2). In this case, $\boldsymbol{X}_b \equiv \boldsymbol{N}$, $\boldsymbol{Y}_b \equiv \boldsymbol{E}$, and $\boldsymbol{Z}_b \equiv \boldsymbol{D}$. Each rate-gyro was then corrupted by drift $\varepsilon_{Xb}=\varepsilon_{Yb}=\varepsilon_{Zb}=2\,°/h$ and additive zero-mean, white noise with standard deviation $\sigma_\varepsilon=1\,°/h$, and integrated between consecutive sensor samples to yield incremental angular measurements. Given the initial position and terrestrial velocity, and ground acceleration $\dot{V}_N, \dot{V}_E, \dot{V}_D$ which the IMU was subject to, the NED ground-truth specific force $\boldsymbol{A}_{sp,NED,t}$ was obtained from Eq. (1). From IMU attitude ground-truth in Eq. (2), $\boldsymbol{D}_b^t \boldsymbol{A}_{sp,NED,t}$ was computed, and each accelerometer corrupted by bias $\nabla_{Xb}=\nabla_{Yb}=\nabla_{Zb}=3mg$ and additive zero-mean, white noise with standard deviation $\sigma_V=1mg$. Integration between consecutive sensor samples resulted in the incremental thrust velocity measurements.

Motion 1 aimed to show whether a constant, long-duration acceleration can enhance observability, though its ultimate velocity is surely not attainable by a low-cost host vehicle. With $\lambda(0)=23°12'S$, $\Lambda(0)=45°52'W$, and $h(0)=600m$ as the initial location at ITA facilities, Motion 1 consisted of constant ground acceleration $a=5m/s^2$ [11][16]:

$$V_N = V_E = -V_D = 300 + at\,[m/s] \qquad t \in [0,200][s] \tag{8}$$

With the same initial location and terrestrial velocity, Motion 2 comprised five PWC, 40s ground acceleration segments as shown in Tab. 1.

TABLE I
MOTION 2 GROUND ACCELERATION SEGMENTS

Segment	$\dot{V}_N$	$\dot{V}_E$	$\dot{V}_D$
1	0	0	0
2	a	0	0
3	0	a	0
4	a	a	0
5	0	0	-a

IV. SIMULATION RESULTS

Making use of solely the indirect feedforward fusion the results showed that the combination of concatenated acceleration maneuvers in distinct directions and rotating the IMU provide accurate estimates. The simulations showed that error propagation of a GINS at rest and in cruise are seen to be similar because of negligible horizontal specific forces in both conditions. Figure 3 shows the ±1–sigma filter–computed standard deviation of the estimation error and one realization of IMU sensor error estimation for Motion 2 combined with IMU rotation. Figure 4 shows the corresponding misalignment. The figures clearly indicate the significant estimation error in the initial acceleration segments, which precluded the use of indirect feedback fusion right from the start for INS reset by means of calibration with estimates of IMU errors and misalignment. Such attempts failed because of filter divergence. The same was observed both for GINS and rotating IMU mechanizations. Thus, switching from feedforward to feedback of error estimates and the corresponding IMU calibration only occurred at $t=195s$. Figure 4 shows how maneuvers improved the misalignment estimation accuracy, notably in azimuth, which is weakly observable when the IMU is stationary on the ground.

After the switch to feedback of error estimates, the INS solution to the attitude DCM computed with Eq. (2) was corrected with the estimated misalignment as follows. Recalling Eq. (4) and Fig. 1:

$$\hat{\boldsymbol{\phi}} = \hat{\boldsymbol{\psi}} + \delta\hat{\boldsymbol{\theta}} \tag{9}$$

$$\hat{\mathbf{D}}_{\mathbf{p}}^{\mathbf{t}} = \begin{bmatrix} 1 & \hat{\phi}_D & -\hat{\phi}_E \\ -\hat{\phi}_D & 1 & \hat{\phi}_N \\ \hat{\phi}_E & -\hat{\phi}_N & 1 \end{bmatrix} \text{ and } \hat{\mathbf{D}}_{\mathbf{t}}^{\mathbf{b}} = \hat{\mathbf{D}}_{\mathbf{t}}^{\mathbf{p}} \mathbf{D}_{\mathbf{p},\mathrm{INS}}^{\mathbf{b}} = (\hat{\mathbf{D}}_{\mathbf{p}}^{\mathbf{t}})^{\mathrm{T}} \mathbf{D}_{\mathbf{p},\mathrm{INS}}^{\mathbf{b}} \tag{10}$$

Throughout the simulation, both before and after switching from feedforward to the feedback configuration the accuracy of the estimated DCM was evaluated by two performance indices. A convergence index J indicated how close the estimated DCM was from the ground-truth, whereas an orthogonality index F measured the degree of orthonormality of the rows (columns) of the estimated DCM:

$$J = \mathrm{trace}\left[\left(\hat{\mathbf{D}}_{\mathbf{t}}^{\mathbf{b}} - \mathbf{D}_{\mathbf{t}}^{\mathbf{b}}\right)^{\mathrm{T}}\left(\hat{\mathbf{D}}_{\mathbf{t}}^{\mathbf{b}} - \mathbf{D}_{\mathbf{t}}^{\mathbf{b}}\right)\right] \geq 0 \tag{11}$$

$$F = \mathrm{trace}\left[\left(\hat{\mathbf{D}}_{\mathbf{t}}^{\mathbf{b}}\hat{\mathbf{D}}_{\mathbf{b}}^{\mathbf{t}} - \mathbf{I}\right)^{\mathrm{T}}\left(\hat{\mathbf{D}}_{\mathbf{t}}^{\mathbf{b}}\hat{\mathbf{D}}_{\mathbf{b}}^{\mathbf{t}} - \mathbf{I}\right)\right] \geq 0 \tag{12}$$

Though not shown here for the sake of space, the statistics of a Monte Carlo simulation with 20 realizations concerning position and velocity estimation errors were indeed encouraging with regard to the novel concept of IFA with a rotating IMU relative to the vehicle. Figure 5 shows a realization of position and velocity errors at the INS output seen in Fig. 2. Feedforward of the error estimates compensate for most errors in the short term. However, errors in the filter model continue to increase due to linearization about the diverging INS output. Filter divergence is avoided by switching to feedback configuration. Then, IMU calibration by means of removal of estimated biases and drifts, and INS reset via correction with estimated misalignment, velocity, and position errors result in a drastic reduction of INS output error. In this condition, the filter model is linearized about a far less incorrect trajectory due to feedback of fairly accurate error estimates, and thus the fusion scheme becomes an extended Kalman filter.

Figure 6 shows the performance indices regarding the computation of the DCM. The results depict a Monte Carlo simulation with 20 realizations, and shows the mean, the minimum, and the maximum values of the respective performance indices. Notice the positive effect of the initial maneuvers on DCM estimation accuracy.

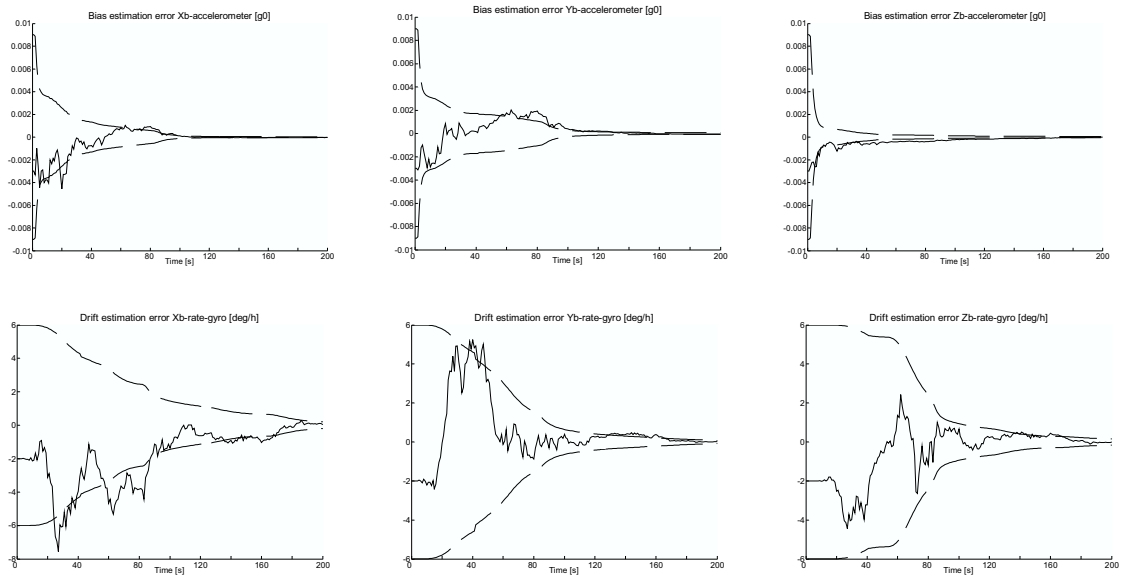

Fig 3. Bias (g_0) and drift (*deg/h*) estimation error − motion 2 and rotating IMU, indirect feedforward fusion.

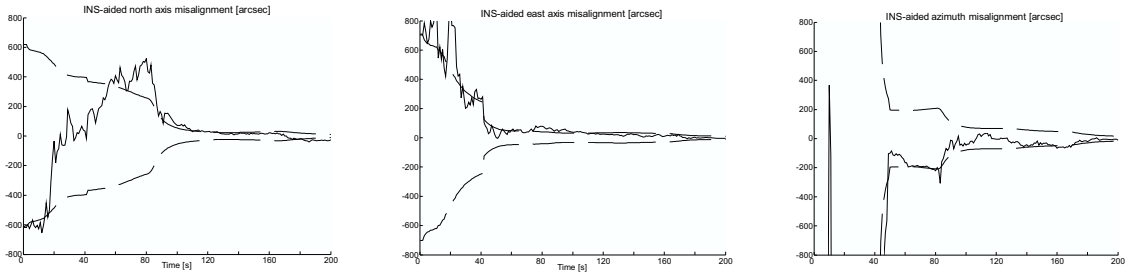

Fig 4. Misalignment estimation error (arcsec) - motion 2 and rotating IMU, indirect feedforward fusion.

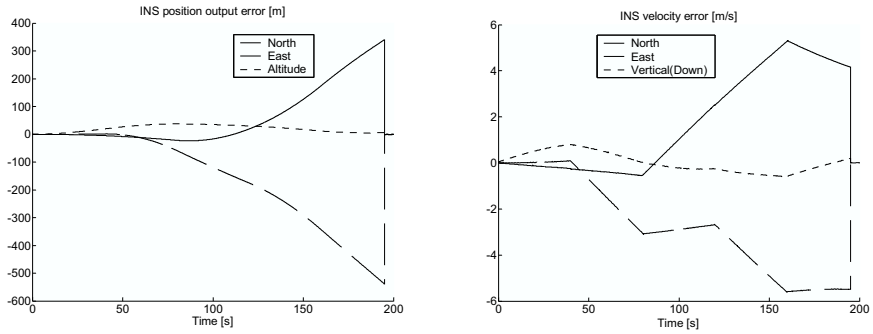

Fig 5. One realization of INS position and velocity output error - motion 2 and rotating IMU – switch at t=195s.

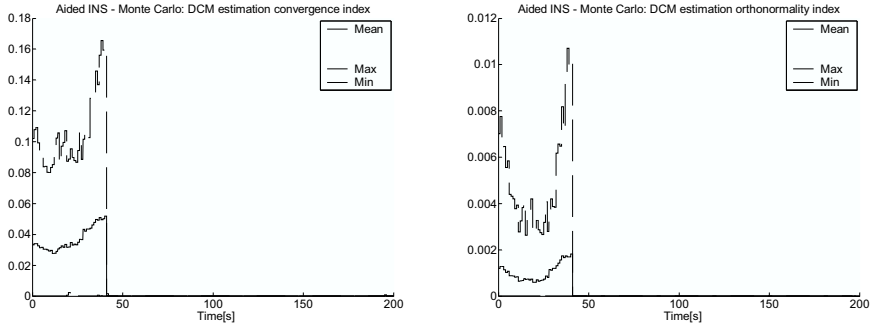

Fig 6. DCM estimation performance indices - motion 2 and rotating IMU – switch at t=195s.

IV. CONCLUSIONS

The results - some not shown here due to limited space - indicated the benefit of continuously rotating the IMU during the stationary initial alignment on the ground at a known location for faster, more accurate estimation of accelerometer bias. The reader is reminded that IMU rotation relative to the host vehicle does not demand the fine engineering, delicate assembly, and accurate moving parts found in a GINS.

Lack of observability caused by insufficient IMU maneuvering produced optimistic filter performance and biased estimation. Such detrimental qualities were mitigated by means of combining IMU rotation with PWC acceleration segments. Improved estimates of accelerometer bias, misalignment - especially in azimuth -, and rate-gyro drift then became available after maneuvers. Then, a switch from feedforward to a feedback configuration took place. On-the-fly IMU calibration and INS reset were then accomplished by way of removing the estimated misalignment, sensor, and navigation errors. The diverging stand-alone INS solution causes model mismatch in the Kalman filter. The indirect feedforward approach with the linearized Kalman filter is only appropriate for short-term applications because model mismatch may cause filter divergence. For long duration applications, the extended Kalman filter arises by means of feedback of error estimates. Caution should be exercised when designing the feedback logic. Switching to feedback mode with full removal of misalignment, accelerometer bias, and rate−gyro drift estimates should only occur *after* the diagonal values of filter covariance **P** decay to safe values determined by simulation to avoid filter divergence.

ACKNOWLEDGEMENTS

The author acknowledges the partial support of project FINEP/FUNDEP/INPE/CTA SIA − Inertial Systems for Aerospace Application. He also hereby expresses his deepest respect to Prof. Itzhack Bar-Itzhack and Prof. Shmuel Merhav, may their memories rest in peace, both late faculty members and research supervisors during my doctorate studies in the Faculty of Aerospace Engineering at the Technion – Israel Institute of Technology.

REFERENCES

[1] A. Adam, E. Rivlin, and H. Rotstein, “Fusion of Fixation and Odometry for Vehicle Navigation”, *IEEE Transactions on Systems, Man, and Cybernetics – Part A: Systems and Humans*, vol. 29, no.6, pp. 593-603, 1999.

[2] S. I. Roumeliotis, A. E. Johnson, and J. F. Montgomery, “Augmenting Inertial Navigation with Image-Based Motion Estimation”, *Proceedings of the IEEE International Conference on Robotics and Automation*, Washington, DC, USA, pp. 4326-4333, 2002.

[3] C. Eck, and H. P. Geering, “Error Dynamics of Model Based INS/GPS Navigation for an Autonomously Flying Helicopter”, *AIAA Guidance, Navigation, and Control Conference*, Denver, CO, USA, pp. 1-9, 2000.

[4] B. H. Hafskjold, B. Jalving, P. E. Hagen, and K. Gade, “Integrated Camera-Based Navigation” *Journal of Navigation*, vol. 52, no. 2, pp. 237-243, 2000.

[5] J. F. Wagner, and T. Wienecke, “Satellite and Inertial Navigation – Conventional and New Fusion Approaches”, Control Engineering Practice, vol. 11, pp. 543-550, 2003.

[6] I. Y. Bar-Itzhack, and N. Berman, “Control Theoretic Approach to Inertial Navigation Systems”, *Journal of Guidance, Control, and Dynamics*, vol. 11, no. 3, pp. 237-245, 1988.

[7] D. Goshen-Meskin, and I. Y. Bar-Itzhack, “Observability Analysis of Piece-Wise Constant Systems with Applications to Inertial Navigation”, *Proceedings of the 29th Conference on Decision and Control*, Honolulu, Hawaii, pp. 821-826, 1990.

[8] J. G. Lee, C. G. Park, and H. W. Park, “Multiposition Alignment of Strapdown Inertial Navigation System”, *IEEE Transactions on Aerospace and Electronic Systems*, vol. 29, no. 4, pp. 1323-1328, 1993.

[9] G.M. Siouris, *Aerospace Avionics Systems: A Modern Synthesis*, Academic Press, San Diego, USA, 1993.

[10] C. Jekeli, “Gravity on Precise, Short-Term, 3-D Free-Inertial Navigation”, *Navigation: Journal of The Institute of Navigation*, vol. 44, no.3, pp. 347-357, 1997.

[11] I. Y. Bar-Itzhack, “Navigation Computation in Terrestrial Strapdown Inertial Navigation System”, *IEEE Transactions on Aerospace and Electronic Systems*, vol. 13, no. 6, pp. 679-689, 1977.

[12] P. G. Savage, “Strapdown Inertial Navigation Integration Algorithm Design Part 2: Velocity and Position Algorithms”, *Journal of Guidance, Control, and Dynamics*, vol. 21, no. 2, pp. 208-211, 1998.

[13] J. Waldmann, “Sculling and Scrolling Effects on the Performance of Multirate Terrestrial Strapdown Navigation Algorithms”, *Proceedings of the 17th International Congress of Mechanical Engineering COBEM2003*, São Paulo, SP, Brazil, ISBN 85-85769-14-9, 2003.

[14] J. Waldmann, “A Derivation of the Computer-Frame Velocity Error Model for INS Aiding”, *Proceedings of the 15th Brazilian Automation Conference (Congresso Brasileiro de Automática)*, Gramado, RS, Brazil, 2004.

[15] Y. Bar-Shalom, and X.-R. Li, *Estimation and Tracking: Principles, Techniques, and Software*, Artech House, Boston, USA, 1993.

[16] I. Y. Bar-Itzhack, “Corrections to Navigation Computation in Terrestrial Strapdown Inertial Navigation System”, *IEEE Transactions on Aerospace and Electronic Systems*, vol. 14, no. 3, pp. 542-544, 1978.